Efficient sorting of Bessel beams

Angela Dudley,[1,*] Thandeka Mhlanga,[1] Martin Lavery,[2] Andre McDonald,[1] Filippus S. Roux,[1] Miles Padgett,[2] and Andrew Forbes[1]

[1]*CSIR National Laser Centre, PO Box 395, Pretoria 0001, South Africa*
[2]*Department of Physics & Astronomy, University of Glasgow, Glasgow, UK*
**adudley@csir.co.za*

Abstract: We demonstrate the efficient sorter of Bessel beams separating both the azimuthal and radial components. This is based upon the recently reported transformation of angular to transverse momentum states. We separately identify over forty azimuthal and radial components, with a radial spacing of 1588 m^{-1}, and outline how the device could be used to identify the two spatial dimensions simultaneously.

OCIS codes: (090.1995) Digital holography; (070.6120) Spatial light modulators; (070.3185) Invariant optical fields; (050.4865) Optical vortices.

References and links

1. M. W. Beijersbergen, L. Allen, H. E. L. O. Van der Veen, and J. P. Woerdman, "Astigmatic laser mode converters and the transferof orbital angular momentum," Opt. Commun. **96**(1-3), 123–132 (1993).
2. J. Arlt and K. Dholakia, "Generation of high-order Bessel beams by use of an axicon," Opt. Commun. **177**(1-6), 297–301 (2000).
3. L. Allen, M. W. Beijersbergen, R. J. C. Spreeuw, and J. P. Woerdman, "Orbital angular momentum of light and the transformation of Laguerre-Gaussian laser modes," Phys. Rev. A **45**(11), 8185–8189 (1992).
4. H. He, M. E. J. Friese, N. R. Heckenberg, and H. Rubinsztein-Dunlop, "Direct observation of transfer of angular momentum to absorptive particles from a laser beam with a phase singularity," Phys. Rev. Lett. **75**(5), 826–829 (1995).
5. A. Mair, A. Vaziri, G. Weihs, and A. Zeilinger, "Entanglement of the orbital angular momentum states of photons," Nature **412**(6844), 313–316 (2001).
6. G. Molina-Terriza, J. P. Torres, and L. Torner, "Management of the angular momentum of light: preparation of photons in multidimensional vector states of angular momentum," Phys. Rev. Lett. **88**(1), 013601 (2002).
7. A. Vaziri, G. Weihs, and A. Zeilinger, "Experimental two-photon, three-dimensional entanglement for quantum communication," Phys. Rev. Lett. **89**(24), 240401 (2002).
8. J. T. Barreiro, T. C. Wei, and P. G. Kwiat, "Beating the channel capacity limit for linear photonic superdense coding," Nat. Phys. **4**(4), 282–286 (2008).
9. J. Leach, B. Jack, J. Romero, A. K. Jha, A. M. Yao, S. Franke-Arnold, D. G. Ireland, R. W. Boyd, S. M. Barnett, and M. J. Padgett, "Quantum correlations in optical angle-orbital angular momentum variables," Science **329**(5992), 662–665 (2010).
10. Z. Bouchal and R. Celechovský, "Mixed vortex states of light as information carriers," New J. Phys. **6**, 131 (2004).
11. R. Celechovský and Z. Bouchal, "Optical implementation of the vortex information channel," New J. Phys. **9**(9), 328 (2007).
12. J. Durnin, J. J. Miceli, Jr., and J. H. Eberly, "Diffraction-free beams," Phys. Rev. Lett. **58**(15), 1499–1501 (1987).
13. J. Turunen, A. Vasara, and A. T. Friberg, "Holographic generation of diffraction-free beams," Appl. Opt. **27**(19), 3959–3962 (1988).
14. A. Vasara, J. Turunen, and A. T. Friberg, "Realization of general nondiffracting beams with computer-generated holograms," J. Opt. Soc. Am. A **6**(11), 1748–1754 (1989).
15. G. Indebetouw, "Nondiffracting optical fields: some remarks on their analysis and synthesis," J. Opt. Soc. Am. A **6**(1), 150–152 (1989).
16. R. P. MacDonald, S. A. Boothroyd, T. Okamoto, J. Chrostowski, and B. A. Syrett, "Interboard optical data distribution by Bessel beam shadowing," Opt. Commun. **122**(4-6), 169–177 (1996).
17. Z. Bouchal, J. Wagner, and M. Chlup, "Self-reconstruction of a distorted nondiffracting beam," Opt. Commun. **151**(4-6), 207–211 (1998).
18. I. Litvin, M. McLaren, and A. Forbes, "A conical wave approach to calculating Bessel-Gauss beam reconstruction after complex obstacles," Opt. Commun. **282**(6), 1078–1082 (2009).
19. M. McLaren, M. Agnew, J. Leach, F. S. Roux, M. J. Padgett, R. W. Boyd, and A. Forbes, "Entangled Bessel-Gaussian beams," Opt. Express **20**(21), 23589–23597 (2012).

#179893 - $15.00 USD Received 13 Nov 2012; revised 13 Dec 2012; accepted 14 Dec 2012; published 2 Jan 2013

20. G. Gibson, J. Courtial, M. J. Padgett, M. Vasnetsov, V. Pas'ko, S. M. Barnett, and S. Franke-Arnold, "Free-space information transfer using light beams carrying orbital angular momentum," Opt. Express **12**(22), 5448–5456 (2004).
21. S. N. Khonina, V. V. Kotlyar, R. V. Skidanov, V. A. Soifer, P. Laakkonen, and J. Turunen, "Gauss–Laguerre modes with different indices in prescribed diffraction orders of a diffractive phase element," Opt. Commun. **175**(4-6), 301–308 (2000).
22. J. Leach, M. J. Padgett, S. M. Barnett, S. Franke-Arnold, and J. Courtial, "Measuring the orbital angular momentum of a single photon," Phys. Rev. Lett. **88**(25), 257901 (2002).
23. M. Lavery, A. Dudley, A. Forbes, J. Courtial, and M. Padgett, "Robust interferometer for the routing of light beams carrying orbital angular momentum," New J. Phys. **13**(9), 093014 (2011).
24. A. F. Abouraddy, T. M. Yarnall, and B. E. A. Saleh, "Angular and radial mode analyzer for optical beams," Opt. Lett. **36**(23), 4683–4685 (2011).
25. I. A. Litvin, A. Dudley, F. S. Roux, and A. Forbes, "Azimuthal decomposition with digital holograms," Opt. Express **20**(10), 10996–11004 (2012).
26. G. C. G. Berkhout, M. P. J. Lavery, J. Courtial, M. W. Beijersbergen, and M. J. Padgett, "Efficient sorting of orbital angular momentum states of light," Phys. Rev. Lett. **105**(15), 153601 (2010).
27. M. P. J. Lavery, G. C. G. Berkhout, J. Courtial, and M. J. Padgett, "Measurement of the light orbital angular momentum spectrum using an optical geometric transformation," J. Opt. **13**(6), 064006 (2011).
28. G. C. G. Berkhout, M. P. J. Lavery, M. J. Padgett, and M. W. Beijersbergen, "Measuring orbital angular momentum superpositions of light by mode transformation," Opt. Lett. **36**(10), 1863–1865 (2011).
29. M. P. J. Lavery, D. J. Robertson, G. C. G. Berkhout, G. D. Love, M. J. Padgett, and J. Courtial, "Refractive elements for the measurement of the orbital angular momentum of a single photon," Opt. Express **20**(3), 2110–2115 (2012).
30. C. López-Mariscal, K. Helmerson; "Shaped nondiffracting beams," Opt. Lett. **35**(8), 1215–1217 (2010).
31. R. Rop, A. Dudley, C. Lopez-Mariscal, and A. Forbes, "Measuring the rotation rates of superpositions of higher-order Bessel beams," J. Mod. Opt. **59**(3), 259–267 (2012).
32. M. P. J. Lavery, D. J. Robertson, A. Sponselli, J. Courtial, N. K. Steinhoff, G. A. Tyler, A. Wilner, and M. J. Padgett, "Efficient measurement of orbital angular momentum over 50 states," New J. Phys. in press.

1. Introduction

Numerous studies have been dedicated to optical fields that carry orbital angular momentum (OAM), where each field has an azimuthal angular dependence of $\exp(il\theta)$ [1–4] where l is the azimuthal index and θ is the azimuthal angle. The fact that these fields offer an unbounded state space has made them advantageous for increasing the amount of information that can be encoded onto a single-photon [5–11]. In particular, higher-order Bessel beams are interesting as OAM-carriers as these fields propagate while maintaining their cross-sectional form over a finite distance [12–15] and reconstruct after encountering an obstacle [16–18]. Recently, entanglement in the Bessel basis has been measured, showing an increased spiral bandwidth [19]. Exploiting these properties of Bessel beams may make them useful in the field of long-range, broad-bandwidth communication systems. However, in order for these fields to be a success in the area of optical communication, efficient techniques for extracting the information they carry need to be demonstrated.

A diffraction grating containing a fork discontinuity can be used to couple light of a particular OAM state into a single-mode fibre [5], but this measurement approach requires that one must test for the chosen range of states sequentially. Attempts to develop more complicated holograms that test multiple states have been made [20, 21], however their efficiency is inversely proportional to the number of states being sampled. An alternative setup that does not alter the OAM state during the measurement procedure is a Mach-Zehnder interferometer with a Dove prism in each arm [22, 23], but to measure 2^n states requires 2^n–1 interferometers. A modified Mach-Zehnder interferometer can also be described to determine both the angular and radial mode content of scalar optical fields [24] but such systems are known to be sensitive to alignment [24]. Digital holograms are also used to extract the azimuthal modal content of optical fields for the reconstruction of its amplitude, phase and OAM density [25]. Recently it has been demonstrated that two spatial light modulators in conjunction with a lens can be used to convert the OAM state of light to a specified lateral position [26–28] so that the azimuthal information may be extracted, while leaving the radial component undefined. The approach has been made more efficient by replacing the spatial light modulators with freeform refractive optical components [29].

#179893 - $15.00 USD Received 13 Nov 2012; revised 13 Dec 2012; accepted 14 Dec 2012; published 2 Jan 2013

In this paper we extend the aforementioned concept to extract the information in both the azimuthal and radial components of Bessel beams. We show that we can identify forty-one OAM states and forty-one radial components of our higher-order Bessel beams, and show the applicability of the approach to measure super-positions of Bessel beams.

2. Concept and experimental setup

In this work we make use of Bessel beams as our OAM-carrying bases functions, which are characterized by an azimuthal mode index, l, and a radial component, k_r, as

$$u(r,\theta,z=0) = J_l(k_r r)\exp(il\theta). \tag{1}$$

Here k_r is the transverse wave number and is defined as $k_r = k\sin\alpha$, where $k = 2\pi/\lambda$ and α is the opening angle of the cone on which the waves propagate. The Fourier transform of the Bessel field is described by an annular ring of radius R,

$$\Im[u(r,\theta)] = \begin{cases} \exp(il\theta) & R \approx r \\ 0 & elsewhere \end{cases}. \tag{2}$$

The radial wavevector is related to the radius of the annular ring as $k_r = kR/f$, where f is the focal length of the Fourier transforming lens. It is these OAM-carrying fields, of differing radial components, whose OAM (l) and radial information (k_r) we wish to measure experimentally.

The technique that is employed for the measurement of the OAM spectrum and the radial components of the Bessel beams consists of two freeform optical elements [29] that map a position in an input plane (x,y) to a position in the output plane (v,u) by a conformal mapping [27–29]

$$v = \frac{d}{2\pi}\arctan\left(\frac{y}{x}\right), \tag{3}$$

$$u = -\frac{d}{2\pi}\ln\left(\frac{\sqrt{x^2+y^2}}{b}\right) = -\frac{d}{2\pi}\ln\left(\frac{k_r f}{kb}\right), \tag{4}$$

where the parameter b controls the scaling of the radial component and d is the aperture size of both freeform optics. An initial radial spacing of Δk_r will result in a vertical spread in the signal plane, Δu, given by

$$\Delta u = \frac{d}{2\pi}\frac{\Delta k_r}{k_r}, \tag{5}$$

and thus the minimum resolvable feature, δ, constrains the resolvable wavevectors to

$$\Delta k_r \geq \frac{2\pi}{d} k_r \delta. \tag{6}$$

This implies that while $\Delta k_r \geq \Delta$ [from Eq. (5)] where Δ is the width of the resulting annular ring, the system is further constrained by δ which is the smallest resolvable feature in the detector plane [from Eq. (6)]. The range of wavevectors that can be detected is also limited by the aperture size of the second freeform optic, $k_r \geq \exp(-\pi)kb/f$.

In this first step an annular ring of light (Fourier transform of the Bessel beam) is mapped to a horizontal line of fixed width, thus any azimuthal phase variation in the ring transforms into a linear phase variation along the line - a tilt of the phase front. If this inclined phase front is passed through a Fourier transforming lens of focal length f, then a focused spot is produced at an l-dependent horizontal position given by

#179893 - $15.00 USD Received 13 Nov 2012; revised 13 Dec 2012; accepted 14 Dec 2012; published 2 Jan 2013

$$\Delta_H = \frac{\lambda f l}{d}. \tag{7}$$

We note that imaging of the output will return the radial information of the field, which is stored in the vertical off-set of the horizontal line of light:

$$\Delta_V = \frac{d}{2\pi}\ln\left(\frac{k_r f}{kb}\right). \tag{8}$$

Thus an optical set-up which images in the vertical axis and Fourier transforms in the horizontal axis will allow the simultaneous measurement of Δ_H and Δ_V and thus the azimuthal and radial information of the field. Such an optical system may be implemented with three cylindrical lenses; a schematic of the concept is given in Fig. 1 with the experimental set-up shown in Fig. 2. A HeNe laser was expanded through a telescope (lenses L1 and L2) to illuminate the liquid crystal display of a spatial light modulator (SLM) where the Bessel beams were encoded in the far-field [Fig. 2(b)] using complex amplitude modulation [30, 31].

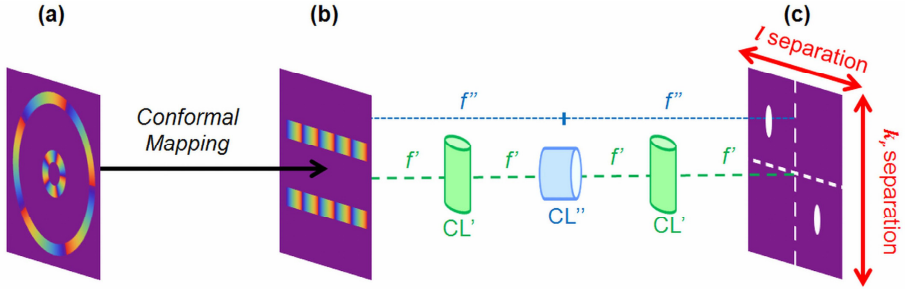

Fig. 1. (a): The annular rings of two Bessel beams are mapped to transverse momentum modes in (b). Cylindrical lenses (CL) arranged in a 4-*f* configuration map the transverse momentum modes to unique *x*- and *y*-coordinates in column (c).

The resulting annular rings were propagated through the mode sorter (denoted by optical elements, R1 and R2), where R1 performed a log-polar mapping thus transforming the azimuthal modes to transverse momentum states, while also mapping the radial component.

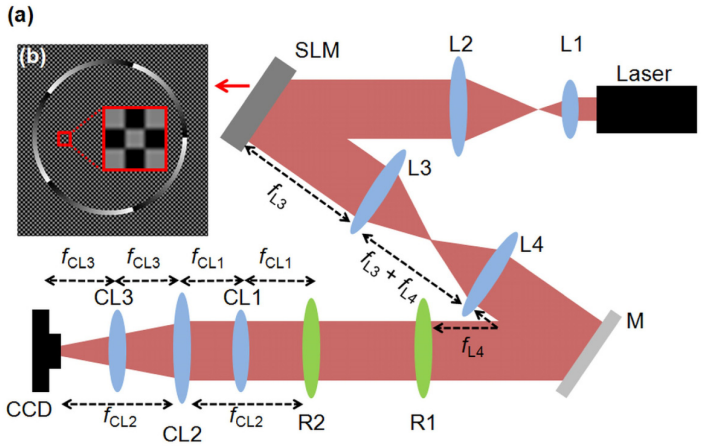

Fig. 2. (a) Schematic of the experimental setup for identifying the azimuthal and radial components of Bessel beams. L, lens (f_{L1} = 15 mm, f_{L2} = 125 mm, f_{L3} = 500 mm, f_{L4} = 500 mm); SLM, spatial light modulator; M, mirror; R, aspheric optical element; CL, cylindrical lens (f_{CL1} = 50 mm,(orientated to focus the *y*-axis), f_{CL2} = 100 mm (orientated to focus the *x*-axis), f_{CL3} = 50 mm (orientated to focus the *y*-axis)); CCD, CCD camera. (b) The phase profile of the annular ring with a zoomed-in insert of the alternating phase values.

#179893 - $15.00 USD Received 13 Nov 2012; revised 13 Dec 2012; accepted 14 Dec 2012; published 2 Jan 2013

The freeform optics were fabricated from PMMA (Poly methyl methacrylate) to an aperture size of d = 16 mm and a focal length of f = 300 mm, with a scaling parameter b = 0.00477. As an illustration, the conformal mapping of the ring into a line is shown as a video clip (Media 1), which contains experimental images of an annular ring ($k_r = 2.62 \times 10^4$ m^{-1}, l = + 1) propagating between the two freeform optical elements.

3. Experimental results and discussion

Bessel beams with $k_r = 2.62 \times 10^4$ m^{-1}, having azimuthal orders ranging from l = –20 to + 20 were generated and directed through the mode sorter. An example of one of the Bessel beams possessing an azimuthal order of l = –5 is given in Fig. 3(a). The unraveled transverse momentum mode at the plane of R2 was focused by a spherical lens having a focal length of f = 250 mm, producing an elongated lateral spot shown in Fig. 3(b). The position of the spots produced by incoming azimuthal modes ranging for l = –20 to + 20 were measured and are given in Fig. 4(a). There is very good agreement between the experimentally measured positions (red circles) and the theoretical expected positions (black curve), calculated from Eq. (7).

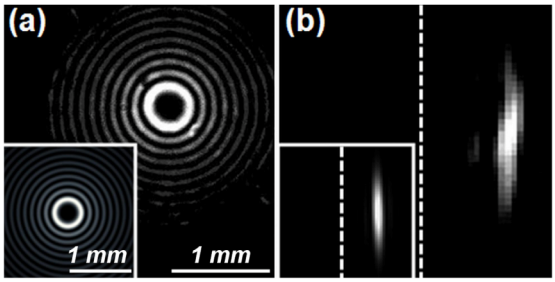

Fig. 3. (a) The Bessel beam and (b) lateral spot for $k_r = 2.62 \times 10^4$ m^{-1} and l = –5. Theoretical results are given as inserts.

The measurement selectivity corresponds to cross-talk between neighboring modes, given by the off-diagonal elements in Fig. 4(b). Our results illustrate that OAM states of higher-order Bessel modes can be measured with a similar selectivity as that obtained for LG modes [26].

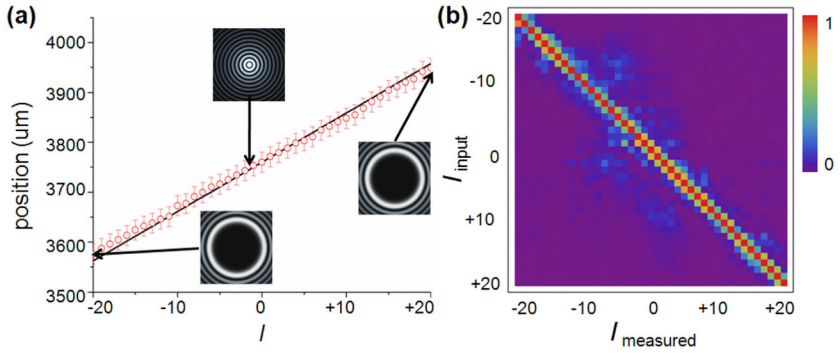

Fig. 4. (a) The position of the spot produced at the plane of the CCD as a function of l. Accompanying theoretical Bessel beams are given as inserts. (b) Relative fractions of the intensity at each detector position for l = –20 to + 20 ($k_r = 2.62 \times 10^4$ m^{-1}). The strong diagonal and weak off-diagonal terms imply a highly accurate and precise mode sorter.

The radial component of the Bessel beam was varied from values of $k_r = 0.23 \times 10^4$ m^{-1} to 6.43×10^4 m^{-1} ($\Delta k_r = 0.16 \times 10^4$ m^{-1}) and an example of one of the Bessel beams is given in Fig. 5(a). In order to simultaneously resolve a range of radial components, the larger of the

#179893 - $15.00 USD Received 13 Nov 2012; revised 13 Dec 2012; accepted 14 Dec 2012; published 2 Jan 2013

two limits [resulting from Eqs. (5) and (6)] needs to be satisfied. For the parameters used in this paper, the radial spacing for two extreme cases (k_r^{max} and k_r^{min}) is constrained by the width of the annular ring ($\Delta k_r \geq 0.32 \times 10^4$ m^{-1}), as well as the smallest resolvable feature in the detector plane ($\delta = 44$ μm): $\Delta k_r \geq 0.11 \times 10^4$ m^{-1}(for $k_r^{max} = 6.43 \times 10^4$ m^{-1}) and $\Delta k_r \geq 0.004 \times 10^4$ m^{-1}(for $k_r^{min} = 0.23 \times 10^4$ m^{-1}). The transformed annular ring was imaged onto the CCD, with the use of two spherical lenses and is depicted in Fig. 5(b). The position of the transformed line shifts vertically as the radius of the annular ring changes and is illustrated in Fig. 6(a), where the measured position of the transformed annular ring is plotted as a function of k_r. Again there is good agreement between the experimentally measured positions (red circles) and the theoretical expected positions (black curve), calculated with the use of Eq. (8). The error bars decrease as the radial component increases because the width of the transformed line in the detector plane becomes narrower.

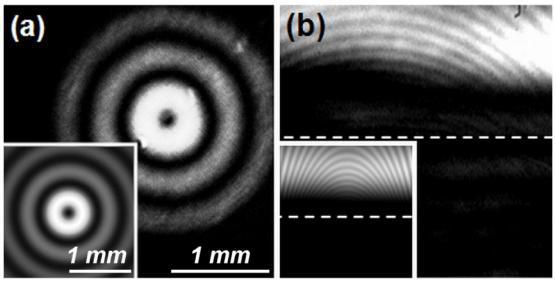

Fig. 5. (a) The Bessel beam and (b) unraveled transverse momentum mode for $l = +1$ and $k_r = 0.72 \times 10^4$ m^{-1}. Theoretical results are given as inserts.

Similarly in detecting the radial components, apertures in the detector plane were centered on the expected line positions and relative fractions of the radial spectrum for various input modes were determined and are presented in Fig. 6(b). Likewise, there is a slight overlap of the transformed lines between neighboring radial coordinates. It is evident from Fig. 6(b) that if this spacing is doubled, the cross-talk between neighboring radial modes will be drastically diminished. Nevertheless, the results of Fig. 4(b) and Fig. 6(b) clearly show that one can extract information stored in both dimensions.

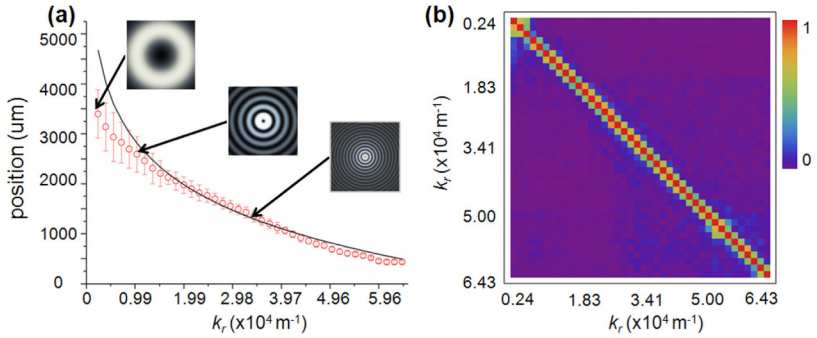

Fig. 6. (a) The position of the transformed line produced at the plane of the CCD as a function of R. Accompanying theoretical Bessel beams are given as inserts. (b) Relative fractions of the intensity at each detector position for $k_r = 0.23 \times 10^4$ m^{-1} to 6.43×10^4 m^{-1} ($l = +1$).

Multiple Bessel beams were also directed through the mode sorter and an example of the superposition Bessel beams is presented in Fig. 7(a). The separation of the two azimuthal and two radial components, when using cylindrical lenses CL1, CL2 and CL3, is depicted in Fig. 7(b) accompanied with the theoretical prediction, illustrating that the mode sorter is capable of distinguishing super-imposed azimuthal and radial modes. Although there is good

#179893 - $15.00 USD Received 13 Nov 2012; revised 13 Dec 2012; accepted 14 Dec 2012; published 2 Jan 2013

agreement between the experimental and theoretical locations of the lateral spots, the shape of the measured lateral spots shows some distortion which could be due to the alignment sensitivity of the cylindrical lenses.

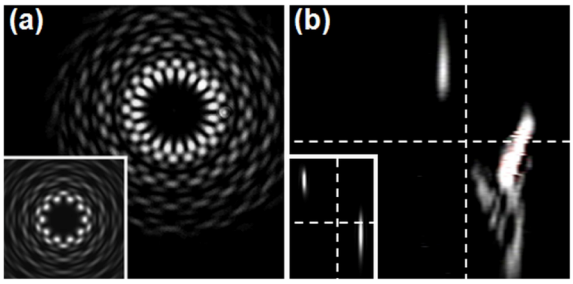

Fig. 7. (a) Super-imposed Bessel beams and (b) the lateral spots produced at the plane of the CCD. Theoretical results are given as inserts.

The number of azimuthal and radial modes that can be identified can be increased by increasing the aperture size of the freeform optical elements. We tested two different aperture sizes (d = 8 mm and 16 mm) and noted that by doubling the aperture diameter, the azimuthal bandwidth that can be identified increased by a factor of 2. Our results could further be improved by first separating the OAM modes into odd and even ports [22, 23] to decrease cross-talk in the measured spectrum.

4. Conclusion

We have illustrated the separation of higher-order Bessel beams in both their azimuthal and radial indices. This technique is not only limited to Bessel beams, but it can also be implemented with other optical fields [32]. The ability to extract encoded information across two higher-dimensional state spaces will prove useful in quantum communication and information systems.

#179893 - $15.00 USD Received 13 Nov 2012; revised 13 Dec 2012; accepted 14 Dec 2012; published 2 Jan 2013